Proceedings of the 10th World Congress on Momentum, Heat and Mass Transfer (MHMT 2025)
Barcelona, Spain – April, 2025
Paper No. CSP 129
DOI: 10.11159/csp25.129

Computational Analysis of Non-Reacting Flow in a Non-Premixed Burner Featuring a Plasma-Enhanced Bluff-Body Swirler

F. Bagherighajari, J.C. Pascoa, M. Abdollahzadehsangroudi
Departamento de Engenharia Eletromecânica, C-MAST – Center for Mechanical and Aerospace Sciences and Technologies, Universidade da Beira Interior
Calçada Fonte do Lameiro, 6201-001 Covilhã, Portugal
f.bagherighajari@ubi.pt ; pascoa@ubi.pt ; mm.abdollahzadeh@ubi.pt

Abstract - This paper presents a novel configuration of a dielectric barrier discharge (DBD) plasma actuator, designed as a plasma swirler and integrated onto the surface of a bluff body in a non-premixed burner. The plasma swirler consists of DBD plasma actuators mounted at 90° in the radial direction, generating plasma-induced ionic wind in the tangential direction. A 3D numerical study of the turbulent, non-reacting flow regime in the combustion chamber is conducted, with the effects of the plasma actuators modelled using a phenomenological approach. Additionally, two alternative configurations of the plasma swirler, inward and outward plasma swirl generators, are analyzed. The study compares the tangential and radial velocity contours and profiles at various axial positions to evaluate the swirl generated by the different configurations. Flow streamlines visualizing the recirculation zones downstream of the bluff body, both with and without the plasma swirler, are also compared. The results demonstrate that the plasma swirler significantly enhances the characteristics of the turbulent recirculation zones. Variations in the swirl number and the spatial mixing index along the axial direction are further analyzed to quantify the impact of the plasma swirl generator on the flow dynamics.

***Keywords*:** Swirl generator, Bluff body burner, flame stabilization, flow control.

1. Introduction

Swirl generation is a typical method for controlling and stabilizing the flame and combustion by enhancing the mixing between the oxidant and the fuel [1]. The behavior of the flow can be altered entirely depending on the level of the swirl. It is also known that the swirling flows can impact the pollutant emissions and flame dynamics, and that processes like blowout and flashback can be controlled by swirling flows [2], [3]. Swirl can be generated conventionally using blades or by injection of the fuel and air with some tangential components inside the combustion chamber. In both cases, the blade and injection angles control the intensity of the swirl generated by the device.

During the last decade, surface dielectric barrier discharge plasma actuators have been used and tested to control fluid flow dynamics in various applications [4]–[6]. Our previous works show that the aerodynamic effect of annular plasma actuators can be used to manipulate the flow and flame characteristics inside a non-premixed burner [7]–[10]. Recently, plasma actuators have generated a swirl for the premixed combustion chamber. Li et al. [11] designed a swirler based on the DBD plasma actuator and demonstrated its effectiveness in jet flow and premixed jet flame control. In their design, the plasma actuators were placed along the axial direction of the injector to induce a circumferential velocity to the main flow, creating a swirl tube. In another work, Li et al. [12] developed a low-swirler injector combining a lobed swirler and a plasma swirler. The lobed swirler was used to enhance the fuel/air mixing downstream of the injector, and the plasma swirler was installed at the injector's exit to control the flame lift-off height. Their results showed that the DBD actuation can be used to adjust the position of the flame front. They have also investigated the effects of electrical parameters on the flow characteristics of their designed plasma swirler [13]. They have also conducted an initial numerical simulation to examine the distribution of the azimuthal velocity and calculate the swirl number. They showed that the swirl number increases almost linearly with the increase of the electrode length until it reaches its maximum at the end of the electrodes. They also showed that at higher applied voltage, the flow divergence tends to be larger, and the flow in the central region is modified, leading to the potential of flow control by adjusting the applied voltage. Li et al. [14] extended their previous research to demonstrate that the central recirculation zone (CRZ) induced by the DBD plasma actuator in a low-swirl burner configuration is the main mechanism by which the plasma swirler influences the flow. When the actuation is on, the CRZ appears as an axisymmetric bubble suspended in the flow, enhancing jet shear layer velocity and increasing flow divergence. This confirms that the plasma swirler's combustion control relies mainly on its aerodynamic effect, modifying the flow field to enhance flame stabilization. Li et al. [15] developed a plasma swirl injector with helical electrodes and compared its performance with the straight electrodes plasma swirler. They showed that this new design can adjust the axial velocity besides the azimuthal velocity and thus can be used to mitigate the flame blow-off or flashback. In the cases mentioned above, the plasma actuator was configured around the peripheral of the inlet tube. The aerodynamic effect of the plasma actuator then results in a tangential flow component. For this purpose, the electrodes of the actuators were aligned in the streamwise direction. The alignment angle of the actuator could also be altered, leading to the so-called helical configuration of the plasma flow swirler.

In the present work, we propose a vanless swirl generator using four DBD plasma actuators mounted in the radial direction on the surface of the DBD plasma actuator. The feasibility of the proposed design will be studied using a three-dimensional simulation of the flow field interaction with the swirl generated by the plasma actuator. The numerical simulation results are presented and discussed in the following sections.

2. Governing equations

The flow governing equations include the continuity, momentum equations described by the time-averaged Navier-Stokes equations, and the species transport equation. We should mention that we have only considered the non-reactive isothermal flow regime inside the combustion chamber. Also, the type of plasma actuator considered is a non-thermal AC DBD plasma actuator, where the thermal power dissipation of the actuator results in negligible temperature variation near the surface of the actuator [16]. In addition, our focus here is only to study the aerodynamic effect of the plasma actuator. Thus, the temperature variation inside the combustion chamber is not considered; overall, the process is assumed to be isothermal. To model the turbulent flow inside the burner, the Low Reynolds Number $k-\varepsilon$ turbulent model has been used. The steady-state governing equations are as follows:

$$\frac{\partial}{\partial x_i}(\rho u_i)=0 \tag{1}$$

$$\frac{\partial}{\partial x_j}(\rho u_i u_j)=-\frac{\partial p}{\partial x_i}+\frac{\partial}{\partial x_j}\left[\mu\left(\frac{\partial u_i}{\partial x_j}+\frac{\partial u_j}{\partial x_i}-\frac{2}{3}\delta_{ij}\frac{\partial u_k}{\partial x_k}\right)\right]+\frac{\partial}{\partial x_j}\left(-\rho\overline{u_i^{'}u_j^{'}}\right)+\overrightarrow{f_b} \tag{2}$$

$$\frac{\partial}{\partial x_i}(\rho u_i Y_k)=-\frac{\partial}{\partial x_i}J_{k,i};\ \ k=CH_4,O_2,N_2 \tag{3}$$

In Equation (2), ρ is the gas mixture density, u_i is the velocity component, p is the pressure, μ is the viscosity and the Reynolds stresses $-\rho\overline{u_i^{'}u_j^{'}}$ is expressed based on the Boussinesq hypothesis as [17] and is evaluated using $k-\varepsilon$ model. In Equation (3), Y_k represents the species mass fraction and $J_{k,i}$ is the diffusion flux of species k. A phenomenological model for the dielectric barrier discharge plasma actuator is adopted here based on the model proposed by Suzen et al. [18], [19]. The governing equations of this model are as follows:

$$\nabla.(\epsilon_r\,\nabla\phi^*)=0 \tag{4}$$

$$\nabla.(\epsilon_r\nabla\rho_c^*)=-\frac{\rho_c^*}{(\lambda_d)^2} \tag{5}$$

In the above, $\phi^*$and ρ_c^* are the normalized electrical potential and charge density and ϵ_r and λ_d are the relative dielectric permittivity and the Debye length. With the solution of these two equations, the plasma-induced body force can be obtained:

$$\vec{f_b}=\rho_c\vec{E}=\rho_c^{max}\phi_{max}f^2(t)\,\rho_c^*(-\nabla\phi^*) \tag{6}$$

3.Results and Discussion

Figure 1 shows the computational grid for the plasma swirler integrated on the bluff body surface. As shown in Figures 1, 1c, 1d, various configuration of the plasma swirler can be made by rotating the electrodes of the plasma actuators around the midline of the electrode length. Actuators can be rotated clockwise and counterclockwise to create inward and outward swirler. The number of the actuators used, and the angle of the rotation can be adjusted to achieve a specific objective.

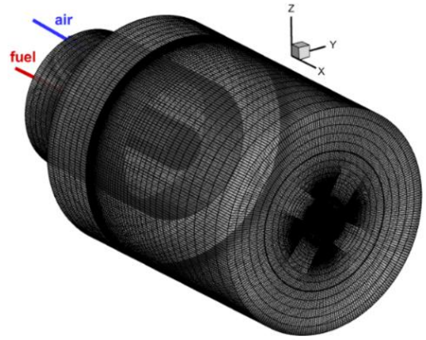

a)

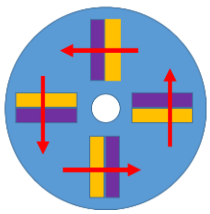

b)

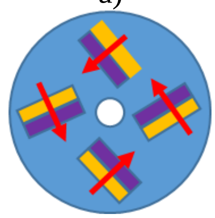

c)

d)

Figure 1: Schematic of the grid and various geometries of the plasma bluff body swirler.

In Figure 2, the contours of the radial velocity components are shown for the case without a plasma actuator, and the results are compared with the case with the normal, inward, and outward plasma swirler. The radial velocity counters are shown in an axial plane with a constant x=5 mm, to show the intensity of the swirl generated by the plasma actuator downstream of the bluff body.

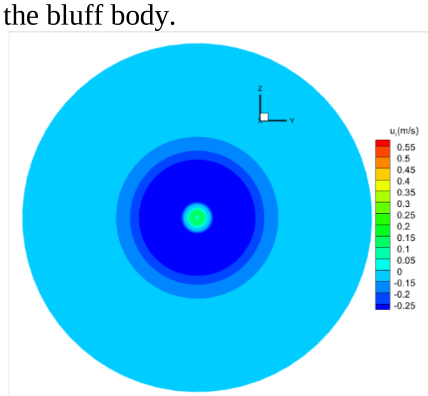

a) without plasma

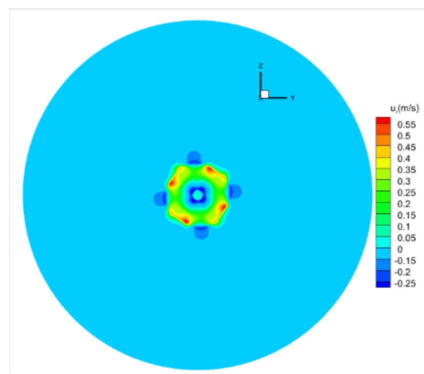

b) base plasma swirler

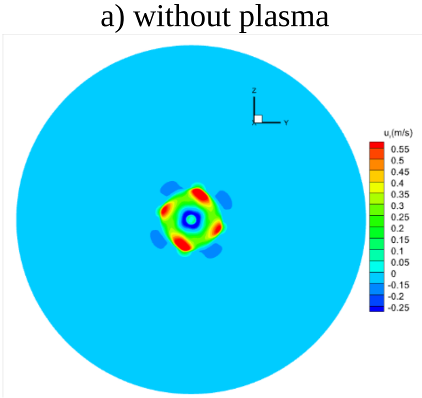

c) inward plasma swirler

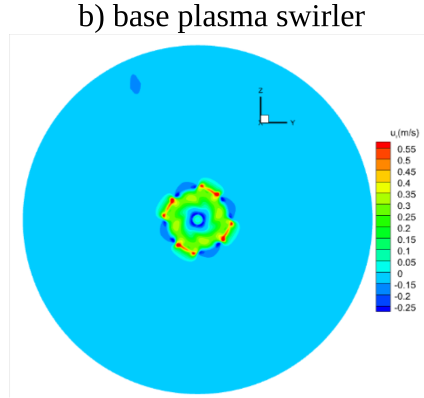

d) outward plasma swirler

Figure 2: contours of the radial velocity at x=10 mm downstream of the bluff body.

In Figure 3, the contours of the tangential velocity components are shown for the case without a plasma actuator, and the results are compared with the case with the normal, inward, and outward plasma swirler. The tangential velocity counters are shown in an axial plane with constant x=5 mm.

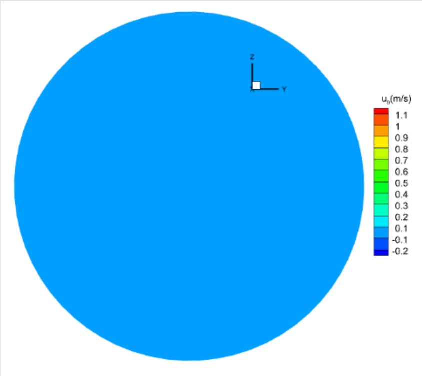

a) without plasma

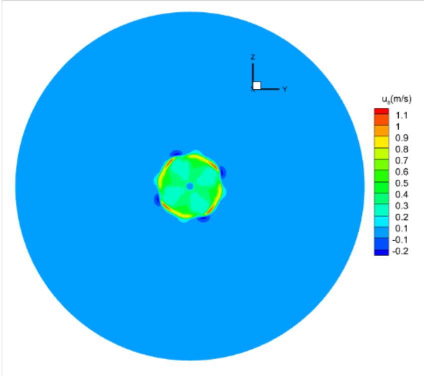

b) base plasma swirler

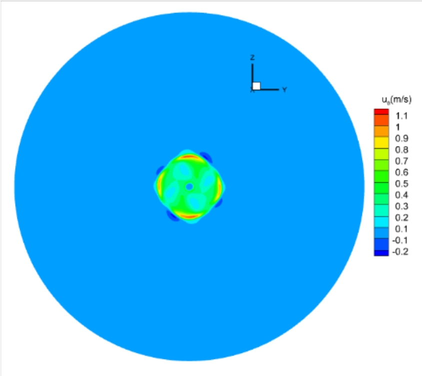

c) inward plasma swirler

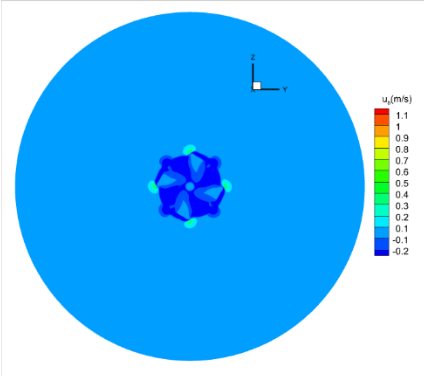

d) outward plasma swirler

Figure 3: contours of the tangential velocity.

In Figure 4, the flow stream lines in the x-y plane drawn at the z=0 and the z-y plane drawn at the x=5mm are shown for the case without plasma actuator, for the case with the normal, inward and outward plasma swirler.

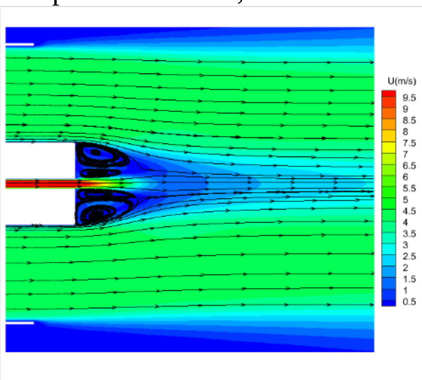

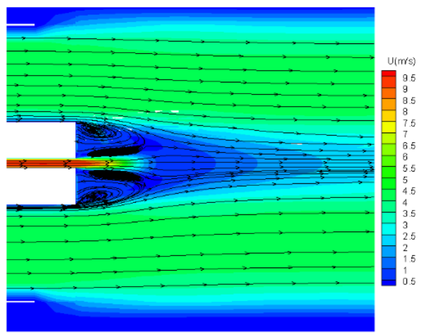

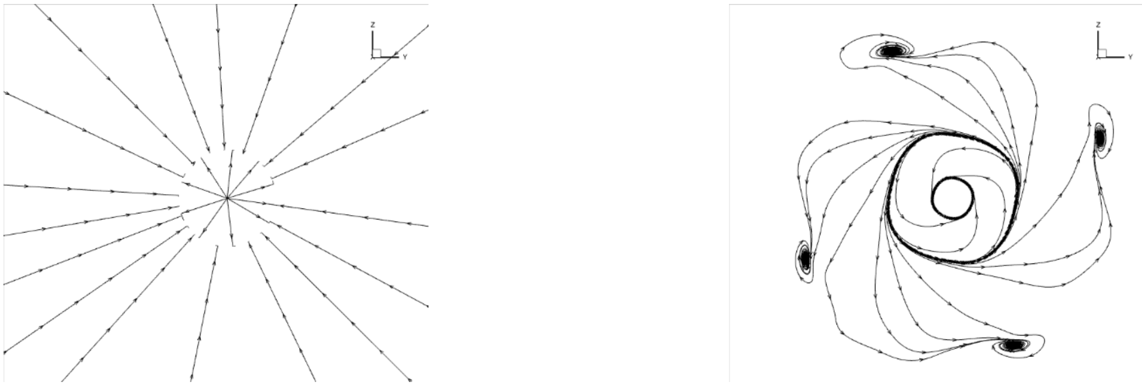

a) without plasma b) base plasma swirler

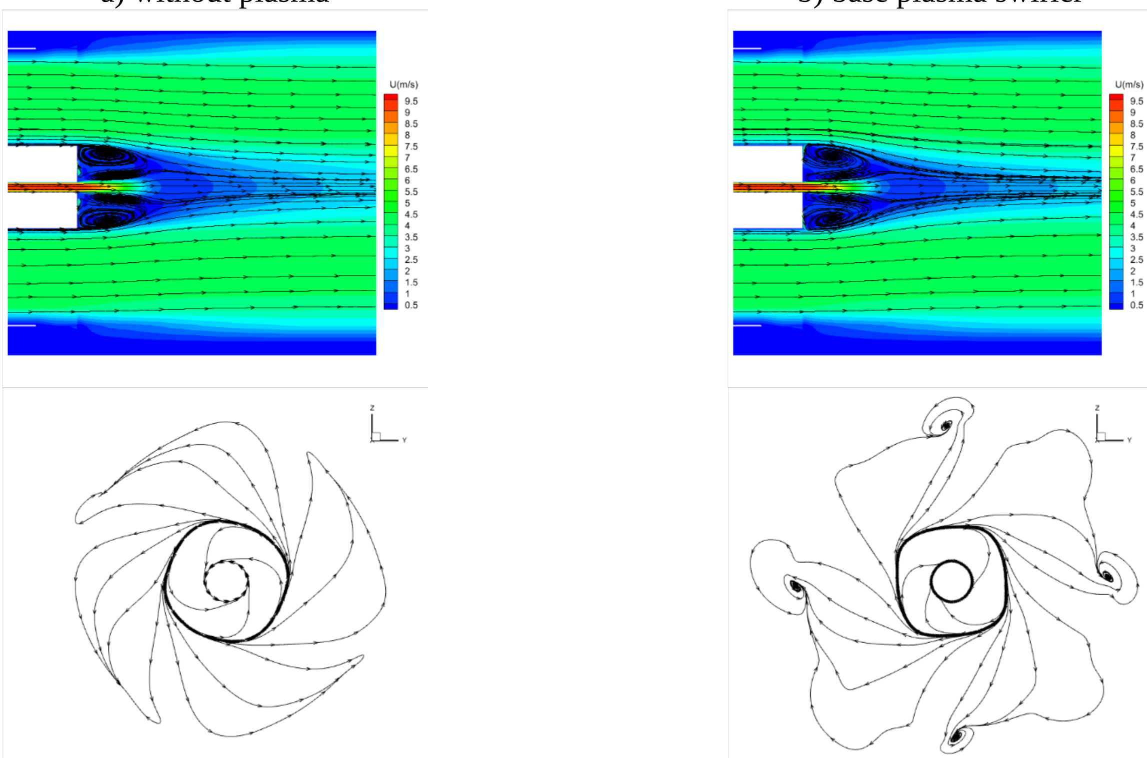

c) inward plasma swirler d) outward plasma swirler

Figure 4: Flow streamlines and velocity contours in the y-x plane.

4. Conclusion

In this work, we have conducted a three-dimensional simulation of the non-reacting flow inside a non-premixed burner equipped with a plasma swirler. The results showed the feasibility of such a device in enhancing the mixing using the velocity contours. The results also showed that the recirculation zones inside the combustion chamber are positively altered.

Acknowledgments

Bagherighajari acknowledges a Ph.D. scholarship with the reference number 2022.09877.BD from FCT-Foundation for Science and Technology, Authors acknowledge the support received within the FCT advanced computing project with the Ref. 2023.10385.CPCA.A0 and the authors also acknowledge the financial support from C-MAST (Center for Mechanical and Aerospace Science and Technology), Research Unit No. 151, Project Grant No. UIDB/00151/2020 (https://doi.org/10.54499/UIDB/00151/2020) and Grant No. UIDP/00151/2020 (https://doi.org/10.54499/UIDP/00151/2020), Funding 2025-2029, transition period

References

[1] J. M. . Beér and N. A. . Chigier, *Combustion aerodynamics*. Halsted Press Division, Wiley, 1972.

[2] D. Feikema, R. H. Chen, and J. F. Driscoll, “Enhancement of flame blowout limits by the use of swirl,” *Combust. Flame*, vol. 80, no. 2, pp. 183–195, May 1990.

[3] A. K. Gupta, J. M. Beér, and J. Swithenbank, “Concentric multi-annular swirl burner: Stability limits and emission characteristics,” *Symp. Combust.*, vol. 16, no. 1, pp. 79–91, Jan. 1977.

[4] F. F. Rodrigues, J. N. Pereira, M. Abdollahzadeh, J. Pascoa, and S. L. Mendez, “Comparative Evaluation of Dielectric Materials for Plasma Actuators Active Flow Control and Heat Transfer Applications,” *Am. Soc. Mech. Eng. Fluids Eng. Div. FEDSM*, vol. 3, Oct. 2021.

[5] M. Abdollahzadeh, F. Rodrigues, J. Nunes-Pereira, J. C. Pascoa, and L. Pires, “Parametric optimization of surface dielectric barrier discharge actuators for ice sensing application,” *Sensors Actuators A Phys.*, vol. 335, p. 113391, Mar. 2022.

[6] M. Sheibani, S. M. M. Jafarian, and M. Abdollahzadehsangroudi, “Impact of annular nanosecond plasma actuators on drag reduction in transonic flow,” *Phys. Fluids*, vol. 36, no. 11, Nov. 2024.

[7] S. Khasare, F. Bagherighajari, F. Dolati, J. Mahmoudimehr, J. Páscoa, and M. Abdollahzadehsangroudi, “The effect of the dielectric barrier discharge plasma actuator in the control of non-reactive flow in a non-premixed bluff body burner,” *Phys. Fluids*, vol. 35, p. 075135, Jul. 2023.

[8] S. Khasare, F. Bagherighajari, F. Dolati, J. Mahmoudimehr, J. C. Pascoa, and M. Abdollahzadeh, “Control of the flame and flow characteristics of a non-premixed bluff body burner using dielectric barrier discharge plasma actuators,” *Appl. Therm. Eng.*, vol. 235, p. 121432, Nov. 2023.

[9] F. Bagherighajari, M. Abdollahzadehsangroudi, and J. C. Páscoa, “Methane/Air Flame Control in Non-Premixed Bluff Body Burners Using Ring-Type Plasma Actuators,” *Actuators 2025, Vol. 14, Page 47*, vol. 14, no. 2, p. 47, Jan. 2025.

[10] F. Bagherighajari, J. Pascoa, and M. Abdollahzadehsangroudi, “Flow Manipulation Strategies: Detached Eddy Simulation Study of DBD Plasma Actuators in a Bluff Body Burner,” in *9th European Congress on Computational Methods in Applied Sciences and Engineering*, 2024, pp. 1–12.

[11] G. Li, X. Jiang, Y. Zhao, C. Li, Q. Chen, G. Xu, and F. Liu, “Jet flow and premixed jet flame control by plasma swirler,” *Phys. Lett. A*, vol. 381, no. 13, pp. 1158–1162, 2017.

[12] G. Li, X. Jiang, J. Zhu, J. Yang, C. Liu, Y. Mu, and G. Xu, “Combustion control using a lobed swirl injector and a plasma swirler,” *Appl. Therm. Eng.*, vol. 152, pp. 92–102, 2019.

[13] G. Li and X. Jiang, “Effects of electrical parameters on the performance of a plasma swirler,” *Phys. Scr.*, vol. 94, no. 9, p. 095601, Jul. 2019.

[14] G. Li, X. Jiang, Z. Lei, C. Liu, J. Yang, Y. Xu, and G. Xu, “Central recirculation zone induced by the DBD plasma actuation,” *Sci. Rep.*, vol. 10, no. 1, pp. 1–9, 2020.

[15] G. Li, X. Jiang, L. Jiang, Z. Lei, J. Zhu, Y. Mu, and G. Xu, “Design and experimental evaluation of a plasma swirler with helical shaped actuators,” *Sensors Actuators A. Phys.*, vol. 315, p. 112250, 2020.

[16] F. Rodrigues, J. Pascoa, and M. Trancossi, “Heat generation mechanisms of DBD plasma actuators,” *Exp. Therm. Fluid Sci.*, vol. 90, pp. 55–65, 2018.

[17] F. G. Schmitt, “About Boussinesq’s turbulent viscosity hypothesis: historical remarks and a direct evaluation of its validity,” *Comptes Rendus - Mecanique*, vol. 335, no. 9–10. pp. 617–627, 2007.

[18] Y. B. Suzen, P. G. Huang, and D. E. Ashpis, “Numerical simulations of flow separation control in low-pressure turbines using plasma actuators,” *Collect. Tech. Pap. - 45th AIAA Aerosp. Sci. Meet.*, vol. 16, pp. 11358–11365, 2007.

[19] M. Abdollahzadeh, J. C. Páscoa, and P. J. Oliveira, “Numerical Modeling of Boundary Layer Control Using Dielectric Barrier Discharge,” in *Conferência Nacional Em Mecânica Dos Fluidos, Termodinâmica e Energia MEFTE*, 2012, pp. Paper No 61, 1–10.